Inorg. Chem. **2007**, *46*, 7944–7952

Pore-Size Tunable Mesoporous Zirconium Organophosphonates with Chiral L-Proline for Enzyme Adsorption

Xin Shi,[†,‡] Jian Liu,[‡] Congming Li,[‡] and Qihua Yang*[,‡]

State Key Laboratory of Catalysis, Dalian Institute of Chemical Physics, Chinese Academy of Sciences, 457 Zhongshan Road, Dalian 116023, China, and Institute of Chemistry for Functionalized Materials, Department of Chemistry, Liaoning Normal University, 850 Huanghe Road, Dalian 116029, China

Received May 9, 2007

Mesoporous zirconium organophosphonates with a tunable mesopore (pore diameter: from 4.8 to 16.3 nm) were synthesized through co-condensation of $ZrCl_4$ and 1-phosphomethylproline (H_3PMP) with the aid of organic additives in the presence of an anionic surfactant (sodium dodecyl sulfate) under weak acidic conditions. The organic additives, tetrahydrofuran, can effectively strengthen the assembly of $ZrCl_4$ and H_3PMP around the surfactant micelles through decreasing the hydrolysis and condensation rate of $ZrCl_4$. The results of the N_2 sorption isotherm and SEM image show that zirconium phosphate with a bimodal structure is formed by calcination of mesoporous zirconium organophosphonate. Mesoporous zirconium organophosphonates can effectively adsorb lysozyme (Lz) and papain, and the adsorption equilibrium for Lz can be reached within 30 min. The adsorption capacity for Lz and papain can reach as high as 438 and 297 mg/g, respectively. Furthermore, Lz adsorbed on mesoporous zirconium organophosphonates can retain its structural conformation as in its free state, and no leaching of Lz from the solid was observed when shaking the Lz-loaded solid in a buffer solution. Also, the existence of L-proline in the mesopore could help the adsorption of papain at a pH value lower than the p*I* of papain.

Introduction

The immobilization of enzymes on insoluble solids, especially adsorption of enzymes on solid supports through physical interactions, is proved to be crucial not only to enhance the stability and durability of enzymes under extreme conditions but also to retain the high activity and stereoselectivity of enzymes in chemical transformations.[1] Moreover, the enzyme immobilization by a physical adsorption method is simple, can be easily operated, and induces fewer modifications in the active conformation of the enzyme because the main driving forces for the adsorption are electrostatic, hydrogen-bonding, and van der Waals interactions.[2,3] Unfortunately, the leaching of the enzymes from the supports is still a bottleneck for the practical application of a supported enzyme in the chemical transformations.[4] Recently, it was reported that zirconium organophosphonates with various surface properties (hydrophilic and/or hydrophobic surfaces) may help to avoid the leaching of the immobilized enzymes due to the enhanced interactions between the enzyme and the solid material.[5] Bellezza et al. systematically investigated the enzyme adsorption behaviors of different kinds of zirconium organophosphonates, such as crystalline layered zirconium phosphate/phosphonate,[6] ZrO_2 nanoparticles modified by phosphoric acid/benzenephosphonic acid,[7] and porous zirconium phosphate/benzenephosphonate.[8] However, in most cases, the amounts of

* To whom correspondence should be addressed. E-mail: yangqh@dicp.ac.cn. Tel: 86-411-84379552. Fax: 86-411-84694447.
† Liaoning Normal University.
‡ Chinese Academy of Sciences.

(1) (a) Klibanov, A. M. *Science* **1983**, *219*, 722. (b) Lalonde, J.; Margolin, A. *Enzyme Catal. Org. Synth. (2nd Ed.)* **2002**, *1*, 163.
(2) (a) Ipson, A. P.; Dunnill, P.; Lilly, M. D. *Biocatalysis* **1990**, *3*, 329. (b) Hamachi, I.; Fujita, A.; Kunitake, T. *J. Am. Chem. Soc.* **1994**, *116*, 8811.
(3) (a) Bosley, J. A.; Clayton, J. C. *Biotechnol. Bioeng.* **1994**, *43*, 934. (b) Znezevic, K.; Mojovic, L.; Adnadjevic, B. *Enzyme Microb. Technol.* **1998**, *22*, 275.
(4) (a) Gill, I.; Ballesteros, A. *Trends Biotechnol.* **2000**, *18*, 282. (b) Schmid, A.; Dordick, J. S.; Hauer, B.; Kiener, A.; Wubbolts, M.; Witholt, B. *Nature* **2001**, *409*, 258. (c) Schoemaker, H. E.; Mink, D.; Wubbolts, M. *Science* **2003**, *299*, 1694.
(5) (a) Kumar, C. V.; Chaudhari, A. *J. Am. Chem. Soc.* **2000**, *122*, 830. (b) Kumar, C. V.; Chaudhari, A. *Chem. Mater.* **2001**, *13*, 238.
(6) (a) Bellezza, F.; Cipiciani, A.; Costantino, U.; Negozio, M. E. *Langmuir* **2002**, *18*, 8737. (b) Bellezza, F.; Cipiciani, A.; Costantino, U. *J. Mol. Catal. B: Enzym.* **2003**, *26*, 47. (c) Bellezza, F.; Cipiciani, A.; Costantino, U.; Nicolis, S. *Langmuir* **2004**, *20*, 5019.

10.1021/ic700892z CCC: $37.00
Published on Web 08/15/2007

immobilized enzyme are not high because of the relatively low surface area and small pore size. Thus, the mesoporous zirconium phosphate/organophosphonate with high surface area and large pore diameter may be desirable host materials for enzymes.

Previous studies show that the synthesis of mesoporous phosphates and organophosphonates through the surfactant-assisted procedure was more difficult than that of mesoporous silica-based materials because of the complex compositions in the synthesis system, i.e., multi-inorganic precursors, surfactant, solvent, and acid or base for adjusting the pH value as well as retaining chemical integrity and porous structure during the process of removing the incorporated template.[9] Until 2003, the "acid−base" route brought forward by Zhao et al. provided an effective method for the synthesis of highly ordered mesoporous phosphates.[10] Unfortunately, the "acid−base" route is not suitable for the synthesis of mesoporous organophosphonates because the organic groups in organophosphonic acid partly decomposed during the calcination step.[11] As far as we know, only a few porous zirconium organophosphonates were synthesized through the surfactant-assisted method.[8,12,13] Therefore, the synthesis of mesoporous zirconium organophosphonates still remains a challenge.

In this paper, we report the one-pot synthesis of the mesoporous zirconium organophosphonates with L-proline in the tunable mesopores by reacting $ZrCl_4$ and the organophosphonate derivative of L-proline, 1-phosphomethylproline (H_3PMP), with the aid of the organic additives in the presence of anionic surfactant. The large and tunable mesopore functionalized with L-proline groups will provide a biocompatible environment for enzymes. Thus, the enzyme adsorption behaviors of these materials were investigated using lysozyme (Lz) and papain as model biomolecules.

2. Experimental Section

General Procedures. 1-Phosphomethylproline (H_3PMP) was prepared by using a modified literature method.[26] Other materials were analytical grade and used as purchased without further purification. Tetrachloride zirconium ($ZrCl_4$, 99.5%) was purchased from Alfa Aesar, and sodium dodecyl sulfate (SDS) was purchased from Changchun Chemical regent. Tetrahydrofuran (THF), NaOH, and triethylamine (TEA) were purchased from Tianjin Chemical regent. Egg white lysozyme (20 000 u/mg) was purchased from Amresco, and papain (200w ∼ 300 wu/g) was obtained from Sanland-chem International Inc.

Synthesis. Mesoporous zirconium organophosphonates functionalized with L-proline were synthesized from tetrachloride zirconium ($ZrCl_4$) and H_3PMP with the aid of organic additives in the presence of an anionic surfactant under weak acid conditions. In a typical synthesis, a mixture of $ZrCl_4$ (5 mmol, 1.165 g) in 5 mL of THF was slowly added to 20 mL of an aqueous solution containing H_3PMP (2.5 mmol, 0.523 g) and desired amounts of SDS under vigorous stirring. Then the pH value of the mixture was adjusted to ca. 4.0 with NaOH (0.5 M, 5 mL) and TEA (12 mmol, 1.21 g). After stirring for 1 h, the mixture was transferred to a Teflon-lined stainless steel autoclave and heated at 160 °C for 24 h. The white powder was filtered off, washed with distilled water, and dried at 60 °C in a vacuum oven. The surfactant was extracted by stirring 1 g of the powder in 80 mL of ethanol containing 1 mL of 2 M HCl at room temperature. The molar ratio of the initial reactants was $SDS:ZrCl_4:H_3PMP:H_2O = n:2:1:556$ ($n = 1$, 2, 4, and 8). The mesoporous zirconium organophosphonates were designated as ^{T}ZrOP-*n*, where *n* ($n = 1$, 2, 4, and 8) is the molar ratio of SDS/H_3PMP in the initial reactants.

The mesoporous zirconium organophosphonate designated as ZrOP-1 was also synthesized in a method similar to that of ^{T}ZrOP-1 but without the addition of THF.

The mesoporous zirconium phosphate, designated as ^{T}ZrP, was obtained by calcining ^{T}ZrOP-2 at 550 °C under an air atmosphere for 2 h.

Characterization. N_2 adsorption−desorption isotherms were obtained at 77 K on Micromeritics ASAP 2010 automated analyzer. The surface areas were estimated according to the Brunauer−Emmett−Teller (BET) method, and the pore-size distributions were calculated based on the Barrett−Joyner−Halenda (BJH) method. Transmission electron microscopy (TEM) was done using a JEM-2010 electron microscope at an acceleration voltage of 120 kV. Scanning electron microscopy (SEM) was performed on a Quanta 200F electron microscope (30 kV). The zirconium and phosphorus contents of the samples were carried out on a Plasma spec-II. ^{31}P (161.8 MHz) MAS NMR spectra were measured on a Bruker DRX-400 spectrometer. The chemical shift of ^{31}P NMR was referenced to $NH_4H_2PO_4$. Fourier transform IR (FT-IR) spectra were recorded on a Thermo Nicolet Nexus 470 FT-IR spectrometer using KBr pellets.

Enzyme Adsorption. Before the adsorption, all solid materials were dried at 80 °C for 24 h in a vacuum oven. A series of standard Lz solutions with concentrations ranging from 1 to 4 mg/mL were prepared by dissolving different amounts of Lz in 100 mL buffer solutions (sodium phosphate, 10 mM, pH = 6.8). In each adsorption experiment, 20 mg of the adsorbents was suspended in 4 mL of the Lz solution with different concentrations. The resulting mixture was continuously shaken in a shaking bath at 293 K for 16 h. The supernatant was separated from the solid materials by centrifugation. The Lz content of the supernatant was measured using UV adsorption at 280 nm. For the kinetic experiments, 20 mg of adsorbent was suspended in 4 mL of a 1.0 mg/mL Lz solution for each measurement.

A series of standard papain solutions with concentrations of 10 mg/mL were prepared by dissolving papain in different buffer solutions (sodium benzoate, 10 mM, pH = 4.0, and sodium borate, 10 mM, pH = 9.2). The adsorption of papain was carried out by mixing 100 mg of the adsorbent in 4 mL of the papain solution, and the mixture was continuously shaken in a shaking bath at 293 K for 16 h. The suspension was then centrifuged, and the supernatant was measured for papain content through the Bradford method on UV spectroscopy ($\lambda = 595$ nm).

(7) Bellezza, F.; Cipiciani, A.; Quotadamo, M. A. *Langmuir* **2005**, *21*, 11099.
(8) Bellezza, F.; Cipiciani, A.; Costantino, U.; Marmottini, F. *Langmuir* **2006**, *22*, 5064.
(9) de A. A. Soler-Illia, G. J.; Sanchez, C.; Lebeau, B.; Patarin, J. *Chem. Rev.* **2002**, *102*, 4093.
(10) (a) Tian, B. Z.; Liu, X. Y.; Tu, B.; Yu, C. Z.; Fan, J.; Wang, L. M.; Xie, S. H.; Stuky, G. D.; Zhao, D. Y. *Nat. Mater.* **2003**, *159*. (b) Yu, C. Z.; Tian, B. Z.; Zhao, D. Y. *Curr. Opin. Solid State Mater. Sci.* **2003**, *7*, 191. (c) Wang, L. M.; Tian, B. Z.; Fan, J.; Liu, X. Y.; Yang, H. F.; Yu, C. Z.; Tu, B.; Zhao, D. Y. *Microporous Mesoporous Mater.* **2004**, *67*, 123.
(11) (a) Kimura, T. *Chem. Mater.* **2005**, *17*, 337. (b) Kimura, T. *Chem. Mater.* **2005**, *17*, 5521.
(12) Ren, N.; Tang, Y.; Wang, Y. J.; Hu, H.; Dong, A. G.; Hua, W. M.; Yue, Y. H.; Shen, J. Y. *Chem. Lett.* **2002**, 1035.
(13) Wu, Z. B.; Liu, Z. M.; Tian, P.; He, Y. L.; Xu, L.; Yang, Y.; Zhang, Y. Y.; Bao, X. H.; Liu, X. C. *Microporous Mesoporous Mater.* **2005**, *81*, 175.

The amount of enzyme adsorbed was calculated by the difference of the concentration of the enzyme before and after adsorption according to the following equation: $M = [C_i V - C_e V]/m$, where M (mg/g) is the amount of adsorbed enzyme per gram of support, C_i (mg/mL) is the initial enzyme concentration, C_e (mg/mL) is the enzyme concentration in the upper limpid solution after adsorption, V (mL) is the volume of the enzyme solution, and m (g) is the weight of the adsorbent.

Isotherm Models. In order to establish the most appropriate adsorption isotherm, the correlation of equilibrium data by either theoretical or empirical models is essential to practical operation. Two isotherm models, Langmuir and Freundlich, were tested in our study. The Langmuir model has several assumptions as follows: adsorption takes place at specific homogeneous sites within the adsorbent; all adsorption sites are identical and energetically equivalent; each site can accommodate only one molecule or atom; there is no interaction between adsorbates. The saturated capacity can be represented by the following expression, where q_e is the solid-phase sorbate concentration at equilibrium (mmol/g), C_e is the sorbate concentration in the aqueous phase at equilibrium (mM), K_L is the Langmuir isotherm parameter (L/g), and a_L is the Langmuir isotherm parameter (L/mmol):

$$q_e = \frac{K_L C_e}{1 + \alpha_L C_e} \tag{1}$$

A linear expression of the Langmuir equation can be represented by

$$\frac{C_e}{q_e} = \frac{1}{K_L} + \frac{\alpha_L}{K_L} C_e \tag{2}$$

Also, K_L/a_L gives the theoretical monolayer saturation capacity (Q_0).

The Freundlich model can be applied to nonideal sorption on heterogeneous surfaces as well as multilayer sorption and is expressed by the following equation:

$$q_e = K_F C_e^{1/n} \tag{3}$$

where q_e is the solid-phase sorbate concentration at equilibrium (mmol/g), C_e is the sorbate concentration in the liquid phase at equilibrium (mM), K_F is the Freundlich parameter [L/(mg$^{1-1/n}$ g)], and $1/n$ (b_F) is the heterogeneity factor. A linear form of the Freundlich expression can be obtained by taking logarithms of eq 4.

$$\ln q_e = \ln K_F + \frac{1}{n} \ln C_e \tag{4}$$

3. Results and Discussion

3.1. Synthesis and Characterization. ZrOP-1 and ^{T}ZrOP-1 were synthesized without and with the addition of THF, respectively. The N_2 adsorption−desorption isotherms of ZrOP-1 and ^{T}ZrOP-1 are shown in Figure 1. The ZrOP-1 sample exhibits a type I isotherm pattern with a sharp N_2 uptake at a relative pressure (P/P_0) above 0.8. The sharp N_2 uptake at a relative pressure above 0.8 and the very broad pore-size distribution of 46 nm indicate the presence of an interparticle pore void. The synthesis of mesoporous zirconium organophophonates (ZrOP) using $ZrCl_4$ as the precursor is very challenging because of the fast hydrolysis and condensation rate of $ZrCl_4$. Generally, the $ZrCl_x(OH)_{4-x}$ species will be formed when $ZrCl_4$ was exposed even in air. The precise control of the hydrolysis and condensation rate of the precursor is one of the key points in the successful synthesis of mesoporous materials using the surfactant-templated method.

With the intention to reduce the chances of self-condensation of $ZrCl_4$, the organic additive, THF, was added. THF, as a polar solvent, can interact with $ZrCl_4$ through an electrostatic force. Thus, the chances of a reaction of $ZrCl_4$ with H_2O for the formation of $ZrCl_x(OH)_{4-x}$ will be reduced. The ^{T}ZrOP-1 sample (synthesized with the addition of THF) presents an isotherm pattern on the border-line between types I and IV with an uncommon type H4 hysteresis loop at P/P_0 between 0.4 and 0.9. The existence of such a type H4 hysteresis loop indicates that some structural defects are formed in the mesoporous framework.[14] The sharp inflection of the isotherm at a relative pressure (P/P_0) above 0.8 also suggests the existence of an interparticle pore void. Compared to ZrOP-1, the narrow pore-size distribution of 4.8 nm can be clearly observed for ^{T}ZrOP-1, suggesting that the addition of an organic additive to the system favors the formation of the mesoporous structure probably through reduction of the hydrolysis and condensation rate of $ZrCl_4$ by THF.

SDS with anionic head groups can interact with Zr^{4+} through electrostatic interaction, which will assist the assembly of $ZrCl_4$ and H_3PMP at the interface of the surfactant micelles for the formation of mesoporous materials. Thus, the influence of the SDS amounts on the structural order of the sample was investigated. ^{T}ZrOP-n (n = 2, 4, and 8) samples synthesized with higher amounts of SDS display a type IV isotherm pattern with a type H2 hysteresis loop, characteristic of mesoporous materials with a uniform mesopore (Figure 1). The TEM image of ^{T}ZrOP-2 clearly shows the existence of a wormlike pore, further confirming that the sample has a disordered mesoporous structure (Figure 2). From ^{T}ZrOP-1 to ^{T}ZrOP-4, the hysteresis loops shift to higher relative pressure (P/P_0), implying an increase of the pore diameter. A pore diameter as large as ~16 nm could be obtained. It is worth noting that an increase of the SDS/H_3PMP ratio above 2 will cause a decrease of the surface area and pore volume (Table 1). All ^{T}ZrOP-n samples exhibit a sharp uptake at a relative pressure of $P/P_0 < 0.1$, suggesting that the samples have a micropore in addition to the mesopore. From the calculation using the t-plot method, we could see that the pore volume derived from the micropore is generally less than 10% of the total pore volume. The results of the N_2 isotherm show that the amounts of SDS employed in the synthesis greatly affect the textural structure of the resultant materials. Through adjustment of the SDS amounts in the initial reactants, the pore diameter of ^{T}ZrOP can be controlled.

A possible formation mechanism of mesoporous zirconium organophosphonates is schematically presented in Figure 3. SDS is one of simplest and most studied anionic surfactants.

(14) (a) Lin, H. P.; Wong, S. T.; Mou, C. Y.; Tang, C. Y. *J. Phys. Chem. B* **2000**, *104*, 8967. (b) Lin, H. P.; Mou, C. Y. *Acc. Chem. Res.* **2002**, *35*, 927. (c) Lin, H. P.; Cheng, Y. R.; Mou, C. Y. *Chem. Mater.* **1998**, *10*, 3772.

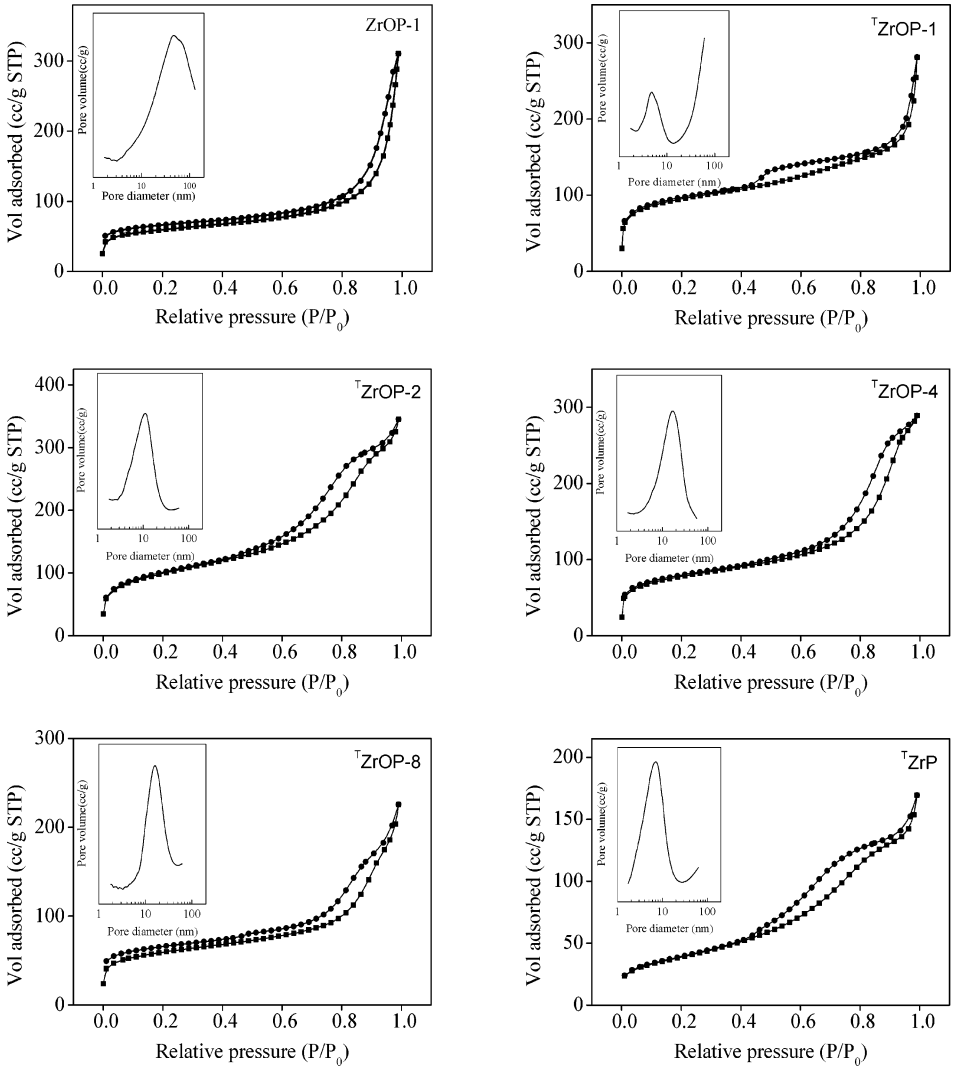

Figure 1. N_2 sorption isotherms of surfactant-extracted ZrOP-1, ^{T}ZrOP-*n* (n = 1, 2, 4, and 8), and ^{T}ZrP (inset shows the pore-size distribution curves).

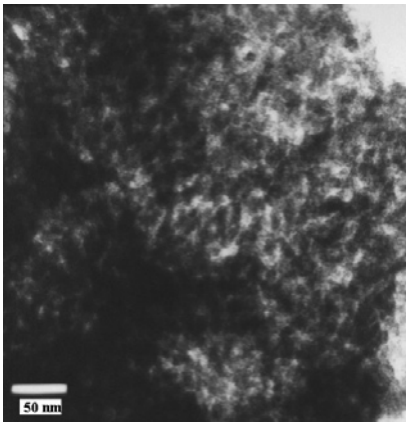

Figure 2. TEM image of ^{T}ZrOP-2.

The anionic surfactant molecules in a water solution are self-organized in micelles with a negatively charged head group. With an increase in the concentration of SDS, the binary system SDS/H_2O presents the phase sequence I (isotropic) → H (hexagonal) → LR (lamellar) with several intermediate mesophases between H and LR, in which all phases show long-range positional order.[15] The addition of salts, cosolvents, and cosurfactants can prodigiously change the size and shape of the micelles.[16] In the present system, H_3PMP is first mixed with SDS. When H_3PMP is added to the solution with a low concentration of SDS, most of the H_3PMP molecules will randomly distribute in the solution because of the limited amounts of micelles (as shown in Figure 3a). When $ZrCl_4$ in THF was added, the reaction of $ZrCl_4$ and H_3PMP may also occur without an interaction with

Table 1. Physicochemical Data for Surfactant-Extracted ZrOP-1, ^{T}ZrOP-*n*, and ^{T}ZrP

	SDS:$ZrCl_4$:H_3PMP	Zr/P	BET surface area (m^2/g)	pore volume (cm^3/g)	pore size BJH (nm)
ZrOP-1	1:2:1		203	0.48	45.6
^{T}ZrOP-1	1:2:1	1.39	328	0.43	4.8
^{T}ZrOP-2	2:2:1	1.41	351	0.53	11.6
^{T}ZrOP-4	4:2:1	1.45	270	0.45	16.1
^{T}ZrOP-8	8:2:1	1.48	205	0.35	16.3
^{T}ZrP	2:2:1	1.13	139	0.26	7.5

[a] ^{T}ZrP is obtained by calcining ^{T}ZrOP-2 at 550 °C to remove the L-proline groups in the material.

(15) (a) Kekicheff, P. *J. Colloid Interface Sci.* **1989**, *131*, 133. (b) Kekicheff, P.; Grabielle- Madelmont, C.; Ollivon, M. *J. Colloid Interface Sci.* **1989**, *131*, 112.
(16) Bergstrom, M.; Pedersen, J. S. *J. Phys. Chem. B* **1999**, *103*, 8502.

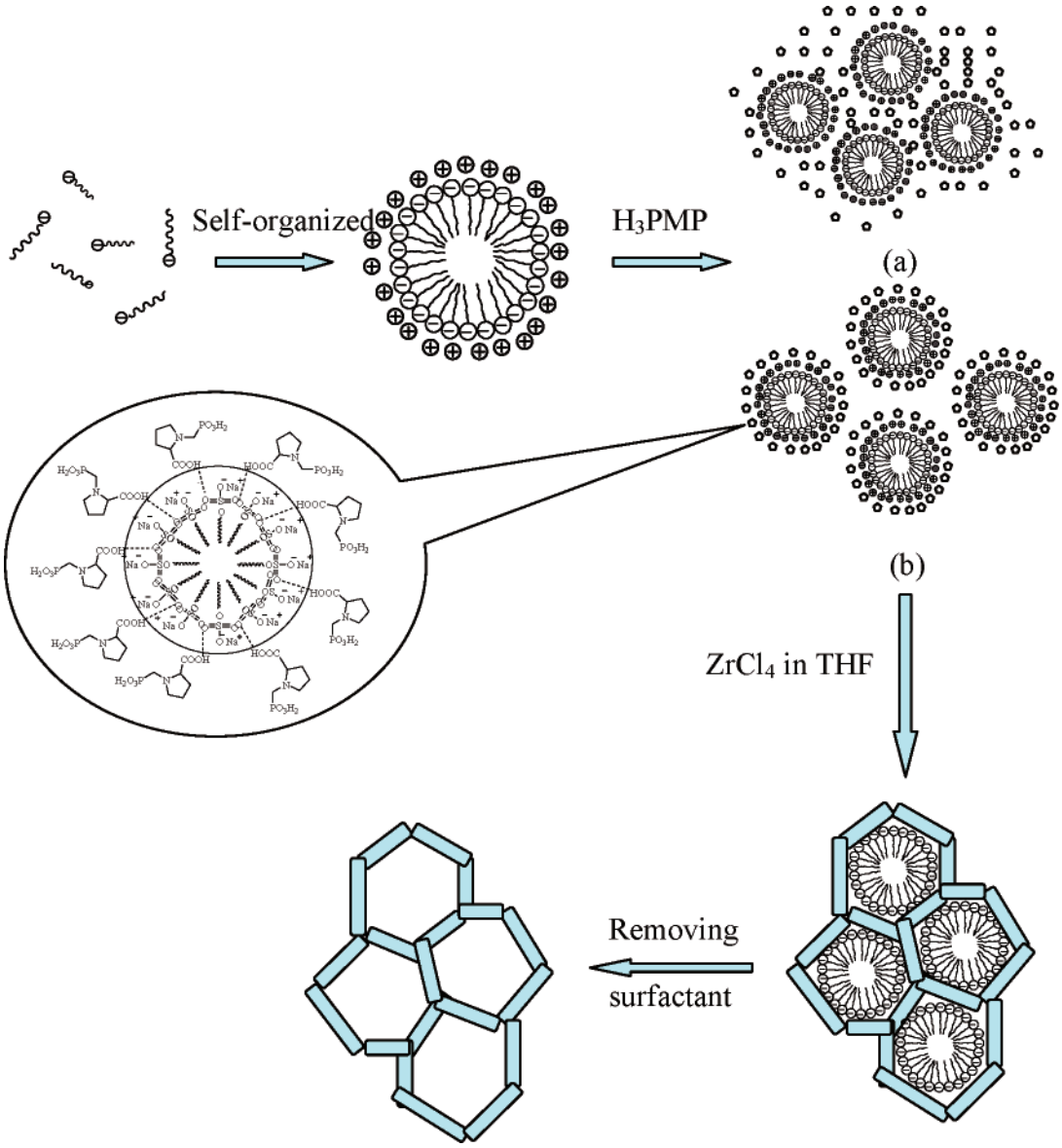

Figure 3. Possible formation mechanism of mesoporous zirconium organophosphonates at pH = 4.0.

the surfactant micelles; therefore, the mesoporous material with a uniform pore-size distribution is difficult to be formed. This can explain the relatively nonuniform pore-size distribution and the existence of an interparticle void in ^{T}ZrOP-1 synthesized with a low concentration of SDS. At a high concentration of SDS, H_3PMP may distribute uniformly at the interface of the micelles through electrostatic interaction or hydrogen bonding (as shown in Figure 3b). $ZrCl_4$ may react with H_3PMP at the interface of the surfactant micelles to form mesoporous materials with a uniform mesopore. With an increase in the amounts of the anionic surfactant in the initial reactants, the size of the micelles also increases in the solution, eventually resulting in the pore-size expansion of the mesoporous materials.[15] However, with a further increase in the SDS concentration, the phase transition from H (hexagonal) to LR (lamellar) may occur, which will lead to the formation of a lamellar-structured material. This can explain the reason that ^{T}ZrOP-8 synthesized with a high concentration of SDS has lower surface area and pore volume compared with ^{T}ZrOP-4 (Table 1). The SEM images show that all samples were irregular blocks constructed from small particles (see the Supporting Information).

The mesoporous zirconium phosphate (^{T}ZrP) was synthesized by calcination of ^{T}ZrOP-2 at 550 °C under an air atmosphere. This sample exhibits also the type IV isotherm pattern, similar to the parent ^{T}ZrOP-2 sample. Compared with ^{T}ZrOP-2, this sample has almost no micropores. The BET surface area, pore diameter, and pore volume are smaller than those of ^{T}ZrOP-2 (Table 1). During the calcination step, further condensation of the framework and reconstruction of the mesoporous structure may occur, which is the main reason for the great change of the textural properties of the sample after calcination. The SEM image shows that ^{T}ZrP has morphologies almost similar to those of the parent ^{T}ZrOP-2 (see the Supporting Information). It is interesting to mention that the mesopores in the range of 20−30 nm can be clearly observed on the bulk particle of ^{T}ZrP (Figure 4). Connected with the result of the N_2 sorption isotherm, we could see that ^{T}ZrP has a bimodal nanostructure with primary and secondary pore diameters of 7.5 and 20−30 nm,

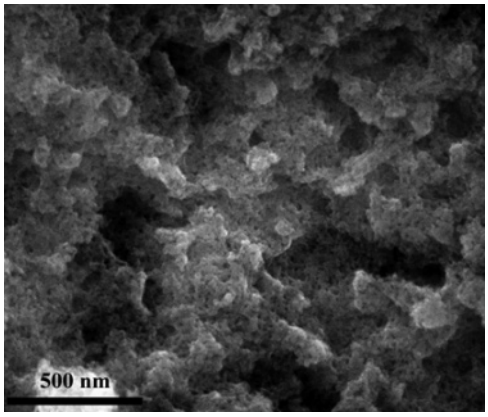

Figure 4. SEM image of TZrP.

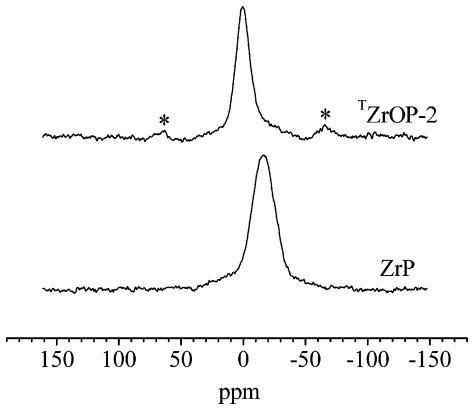

Figure 5. ^{31}P MAS NMR spectra of surfactant-extracted TZrOP-2 and TZrP.

respectively. The existence of the bimodal pore structure is favorable for the mass transfer of the guest molecules within the mesopore of the sample. The formation of the secondary mesopore is probably due to the decomposition of organic groups and the reconstruction of the mesostructure during the calcination step. The mesoporous zirconium phosphate with hierarchical mesopores can be obtained through calcination of the mesoporous zirconium organophosphonate.

The spectra of ^{31}P MAS NMR, as shown in Figure 5, present the status of phosphorus species in the framework of TZrOP-*n* and TZrP. TZrOP-2 displays a peak centered at 0 ppm, which could be assigned to organic phosphorus species.[17] TZrP shows a broad peak at −17 ppm, which can be assigned to the inorganic phosphorus species, tetrahedral phosphorus atoms bonded to four or less ZrO_4 units, according to the previous references.[18,19] Tetrahedral zirconium and tetrahedral phosphorus alternately arranged may present in the framework of TZrP after removal of the L-proline groups by calcination. The results of ^{31}P MAS NMR spectra confirm the incorporation of organophosphonate groups into TZrOP-*n*. In general, the ratio of Zr/P for crystalline zirconium phosphates (including α-ZrP and γ-ZrP) is 1:2.[20] The Zr/P ratio of the mesoporous zirconium organophosphonates is in the range of 1.39−1.48, independent of the Zr/P initial ratio of 2 (Table 1). The Zr/P ratio in the solid sample is lower than that in the initial composition, suggesting that zirconium is not stoichiometrically incorporated. The Zr/P ratio of TZrP is 1.13, which is lower than that of the parent TZrOP-2. This may result from a further reaction between the zirconium and phosphorus species during the calcination step.

3.2. Enzyme Adsorption. The dimension of Lz is 3.0 × 3.0 × 4.5 nm^3, and the isoelectric point (p*I*) is around 11.0.[21,22] To establish the most appropriate adsorption isotherm, Langmuir and Freundlich models were tested in this text. The adsorption data were analyzed according to the linear form of the Langmuir equation (eq 2). Figure 6 shows the plots of the specific sorption (C_e/q_e) against C_e for TZrOP-*n* (n = 1, 2, 4, and 8). It is clear from Figure 6 that the Langmuir model is not suitable for describing the adsorption behavior of TZrOP-1 because of the poor correlation coefficients. In contrast, the correlation coefficients of TZrOP-*n* except for TZrOP-1 are extremely high, and the isotherms are linear over the whole concentration range. This shows that the Langmuir isotherm can accurately describe the adsorption behaviors of TZrOP-*n* (n = 2, 4, and 8). Table 2 presents the isotherm parameters (K_L and a_L), the correlation coefficients (R^2), and the equilibrium monolayer capacities (Q_0). High values of a_L indicate a strong interaction between Lz and the support, TZrOP-*n* (n = 2, 4, and 8).

The adsorption data were also analyzed according to the linear form of the Freundlich equation (eq 4). Figure 7 displays the logarithmic plots of the Freundlich equation for TZrOP-*n*. It can be seen obviously that the adsorption behavior of TZrOP-1 can be well described using the Freundlich equation (eq 4). The correlation coefficient is extremely high, and the isotherm is linear over the whole concentration range, whereas there is a rather large deviation from linearity for TZrOP-*n* except for TZrOP-1 in the whole concentration range, indicating that the experimental data for TZrOP-*n* (n = 2, 4, and 8) do not fit the Freundlich model. Table 3 lists the Freundlich sorption isotherm parameters b_F, K_F, and the correlation coefficients R^2 for TZrOP-*n*.

On the basis of the analysis described above, it can be seen that the Langmuir isotherm can accurately describe the adsorption behaviors of TZrOP-*n* (n = 2, 4, and 8) while the Freundlich isotherm can accurately describe the adsorption behaviors of TZrOP-1. The adsorption isotherms of Lz onto TZrOP-*n* employing the appropriate model are shown in Figure 8. The solid line for TZrOP-1 represents a fit of the experimental data by employing the Freundlich model, and other solid lines for TZrOP-*n* (n = 2, 4, and 8) display a fit of the experimental data by employing the Langmuir model. The adsorption isotherms of TZrOP-2, TZrOP-4, and TZrOP-8 display a sharp uptake followed by a well-defined plateau, indicating a high affinity between Lz and the samples. This

(17) Shi, X.; Yang, J.; Yang, Q. H. *Eur. J. Inorg. Chem.* **2006**, 1936.
(18) Sayari, A.; Moudrakovski, I.; Reddy, J. S.; Ratcliffe, C. I.; Ripmeester, J. A.; Preston, K. F. *Chem. Mater.* **1996**, *8*, 2080.
(19) Tiemann, M.; Schulz, M.; Jäger, C.; Fröba, M. *Chem. Mater.* **2001**, *13*, 2885.
(20) Alberti, G.; Casciola, M.; Costantino, U.; Vivani, R. *Adv. Mater.* **1996**, *8*, 291.
(21) Kharakoz, D. P.; Sarvazyan, A. P. *Biopolymers* **1993**, *33*, 11.
(22) Wilson, K. P.; Malcolm, B. A.; Matthews, B. W. *J. Biol. Chem.* **1992**, *267*, 10842.

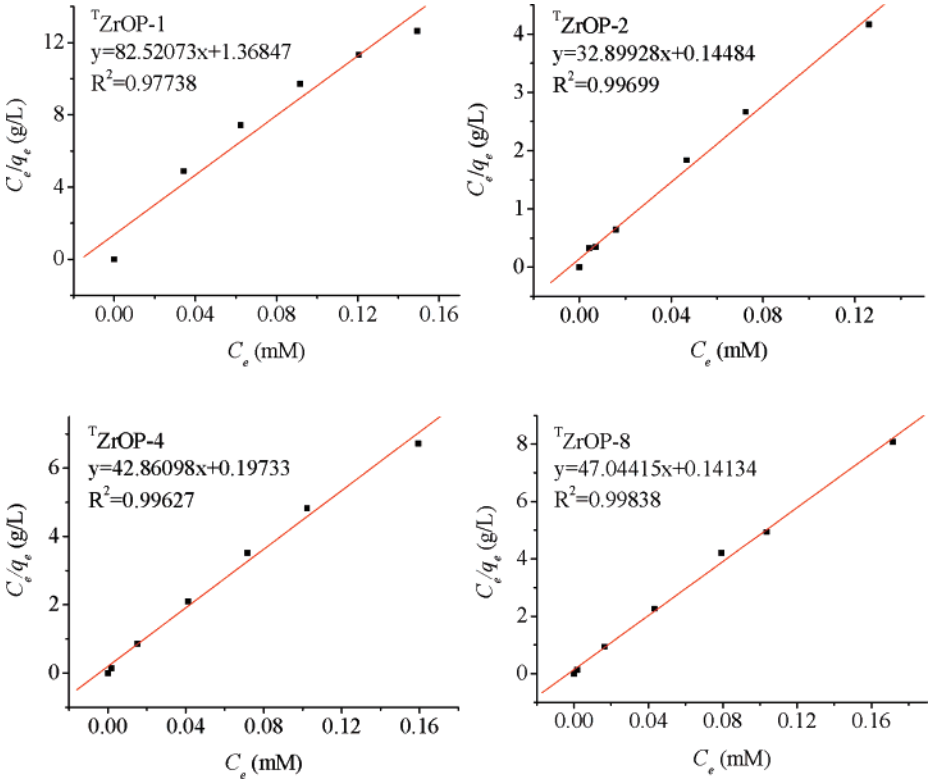

Figure 6. Langmuir isotherm linear plots for the sorption of Lz onto ^{T}ZrOP-*n* (*n* = 1, 2, 4, and 8).

Table 2. Langmuir Sorption Isotherm Parameters for ^{T}ZrOP-*n* (*n* = 1, 2, 4, and 8)

	K_L (L/g)	a_L (L/mmol)	R^2	Q_0 (mg/g)
^{T}ZrOP-1	0.7307	60.30	0.977 38	175
^{T}ZrOP-2	6.9042	227.14	0.996 99	438
^{T}ZrOP-4	5.0677	217.20	0.996 27	336
^{T}ZrOP-8	7.0759	332.84	0.998 38	306

can be supported by their high a_L values, as shown in Table 1. ^{T}ZrOP-1 exhibits a lower binding affinity for Lz than ^{T}ZrOP-*n* (*n* = 2, 4, and 8) does. ^{T}ZrOP-1 has a relatively high surface area compared with ^{T}ZrOP-*n* (*n* = 4 and 8). The pore size of this sample is 4.8 nm, which is large enough for accommodation of Lz with dimensions of 3.0 × 3.0 × 4.5 nm^3. Its low binding affinity for Lz may be explained by the pore-blocking effects of the small pore. ^{T}ZrOP-2 exhibits the highest Lz saturation adsorption capacity among all of the samples investigated because of its high surface area, large pore volume, and uniformly distributed pore size.

The kinetics of adsorption for ^{T}ZrOP-*n* (*n* = 1, 2, 4, and 8) are presented in Figure 9. ^{T}ZrOP-1, ^{T}ZrOP-2, and ^{T}ZrOP-4 can reach equilibrium within 30 min, suggesting that these new kinds of adsorbents show fast adsorption rates. Though ^{T}ZrOP-8 exhibits a slower adsorption rate, equilibrium can still be obtained in 1 h. The difference between ^{T}ZrOP-8 and the other ^{T}ZrOP-*n* samples is mainly due to its lower surface area and pore volume. ^{T}ZrOP-*n* with fast adsorption rates may have potential applications in view of the fast immobilization and separation of biomolecules.

The conformation of Lz adsorbed onto ^{T}ZrOP-2 was investigated by FT-IR spectroscopy (Figure 10). In general, the bands of amide I and amide II are employed to study the protein structure because these two bands are sensitive to the protein structural change. The amide band I near 1650 cm^{-1} is assigned to the stretching vibration of the carbonyl coupled to C−N, and the amide band II near 1550 cm^{-1} is attributed to the bending and stretching of N−H and C−N vibrations.[23] For Lz, the amide bands I (1653 cm^{-1}) and II (1533 cm^{-1}) are due to the α-helical confirmation and the parallel *β*-sheet structure, respectively.[24,25] The FT-IR spectrum of ^{T}ZrOP-2 displays the carbonyl vibrations of COO$^-$ at 1630 cm^{-1} and the COOH vibration of the L-proline group at 1730 cm^{-1}. The broad band in the range of 1300−1500 cm^{-1} can be attributed to C−H vibrations of the pyrrolidine ring of the L-proline group. After Lz adsorbed onto ^{T}ZrOP-2, the amide band I (1653 cm^{-1}) and the amide band II (1533 cm^{-1}) of Lz still can be obviously observed, indicating that Lz retains its structural conformation. The COO$^-$ vibration band at 1630 cm^{-1} and the COOH vibration band at 1730 cm^{-1} of L-proline in ^{T}ZrOP-2 were overlapped with the amide band I (1653 cm^{-1}) of Lz. The results of FT-IR confirm that the adsorption of Lz onto ^{T}ZrOP-*n* does not lead to a denaturation of the enzyme.

The leaching degree of the enzyme physically immobilized on the solid product is very important for further application. Therefore, we investigated the stability of Lz on ^{T}ZrOP-*n* by shaking the Lz-loaded sample in a buffer solution with different pH values. After 16 h, the liquid was taken out and the Lz content in the supernatant was measured. For all

(23) Hammond, W.; Prouze, E.; Mahanti, S. D.; Pinnavaia, T. J. *Microporous Mesoporous Mater.* **1999**, *27*, 19.
(24) Adams, S.; Higgins, A. M.; Jones, R. A. L. *Langmuir* **2002**, *18*, 4854.
(25) Vinu, A.; Murugesan, V.; Hartmann, M. *J. Phys. Chem. B* **2004**, *108*, 7323.
(26) Turner, A.; Jaffrès, P. A.; MacLean, E. J.; Villemin, D.; Mckee, B.; Hix, G. B. *J. Chem. Soc., Dalton Trans.* **2003**, 1314.

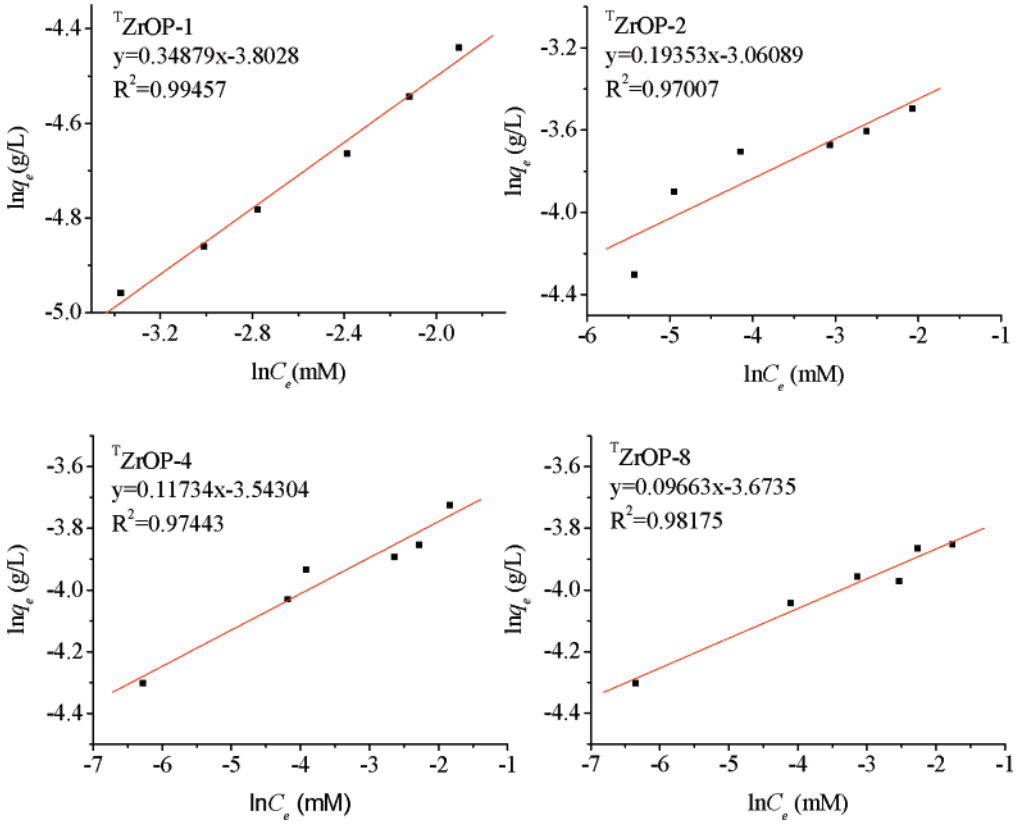

Figure 7. Freundlich isotherm linear plots for the sorption of Lz onto ^{T}ZrOP-*n* (*n* = 1, 2, 4, and 8).

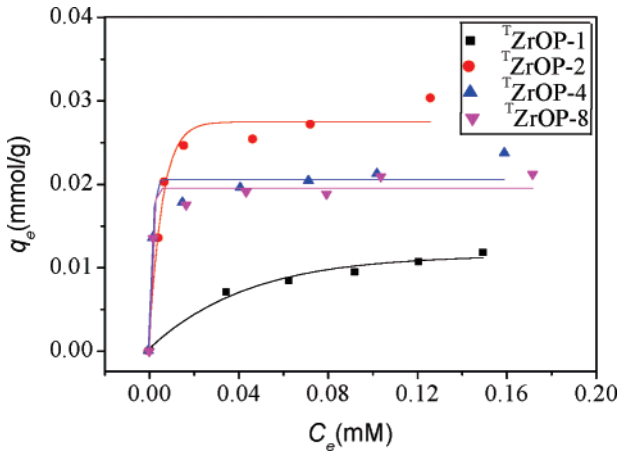

Figure 8. Adsorption isotherms of Lz onto ^{T}ZrOP-*n* (*n* = 1, 2, 4, and 8) (phosphate buffer, pH = 6.8, *t* = 16 h, *T* = 25 °C).

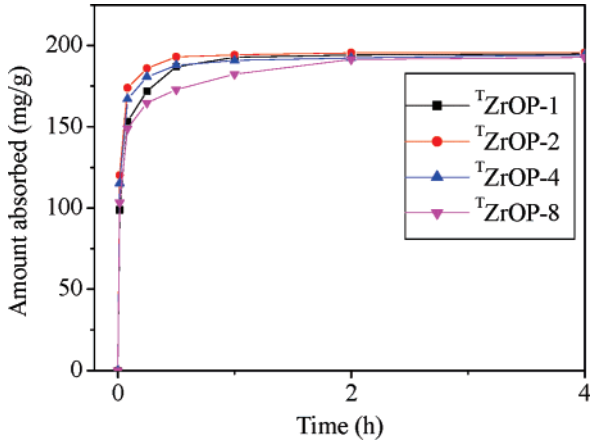

Figure 9. Kinetics of the adsorption of ^{T}ZrOP-*n* (*n* = 1, 2, 4, and 8) (200 mg of Lz/g of support, phosphate buffer, pH = 6.8, *t* = 16 h, *T* = 25 °C).

Table 3. Freundlich Sorption Isotherm Parameters for ^{T}ZrOP-*n* (*n* = 1, 2, 4, and 8)

	b_F	K_L [L (mg$^{1-1/n}$ g)]	R^2
^{T}ZrOP-1	0.348 79	0.022 38	0.994 57
^{T}ZrOP-2	0.193 53	0.046 85	0.970 07
^{T}ZrOP-4	0.117 34	0.028 93	0.974 43
^{T}ZrOP-8	0.096 63	0.025 39	0.981 75

samples, almost no leaching of Lz from the solid samples was observed, as is evidenced by the fact that only about 0.1% of Lz was detected in the supernatant. The high affinity of ^{T}ZrOP-*n* to Lz may be related with the existence of L-proline groups in the mesopore, which will provide more anchoring and interaction sites for Lz.

The influence of the pH value on the adsorption behavior of ^{T}ZrOP-*n* was compared with ^{T}ZrP using papain as model biomolecules. The isoelectric point (p*I*) of papain is 8.75. The pH values of 4.0, 6.8, and 9.2 were employed in the experiments. The amounts of papain adsorbed onto ^{T}ZrOP-*n* and ^{T}ZrP at different pH values are shown in Figure 11. It can be observed clearly that the adsorption capacity for papain decreases with an increase in the pH value. Also, the adsorption capacities of ^{T}ZrOP-*n* samples are much higher at pH = 4.0 than at pH = 9.2. At pH = 4.0, the papain is positively charged. The the pH is increased to 9.2, the papain is negatively charged. The surface of ^{T}ZrOP-*n* rich in POH groups is negatively charged in the range of the pH value from 4.0 to 9.2. Moreover, H_3PMP in the mesopore of

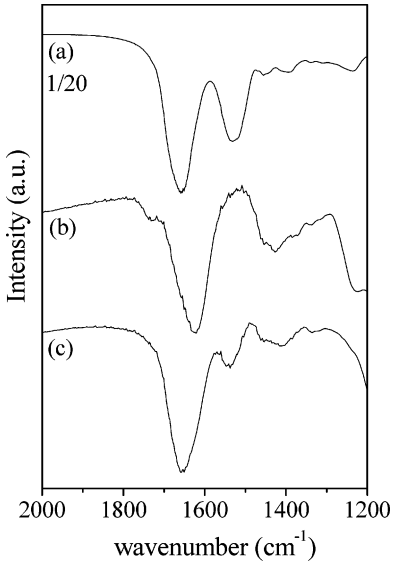

Figure 10. FT-IR spectra of (a) free Lz, (b) ^{T}ZrOP-2, and (c) ^{T}ZrOP-2 loaded with Lz.

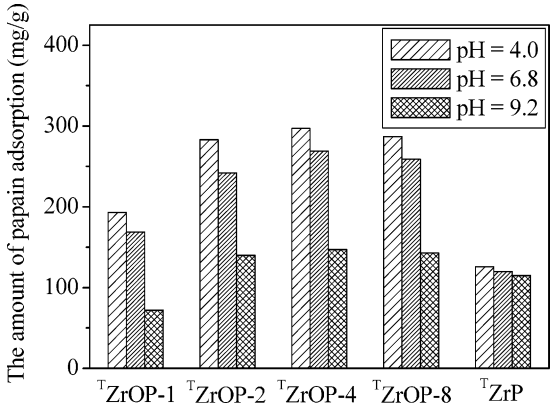

Figure 11. Amount of papain adsorbed onto ^{T}ZrOP-*n* (n = 1, 2, 4, and 8) and ^{T}ZrP at different pH values (100 mg of supports in 4 mL of papain of 10 mg/mL).

^{T}ZrOP-*n* is also negatively charged at this pH range. Therefore, the repulsion of the negatively charged papain and ^{T}ZrOP-*n* results in lower adsorption amounts of papain at pH = 9.2 than at pH = 4.0. Thus, the main driving force for the papain adsorption onto ^{T}ZrOP-*n* is the electrostatic interactions. However, the ^{T}ZrP sample exhibits only slightly higher adsorption amounts at pH = 4.0 than at pH = 9.2. The ^{T}ZrOP-*n* samples have L-proline in the mesopore. ^{T}ZrP was formed by calcination of ^{T}ZrOP-2 in an air atmosphere; thus, no L-proline exists in the mesopore of ^{T}ZrP. At pH = 9.2, the repulsion of negatively charged papain and ^{T}ZrP is weaker because of the less amounts of negative charge of ^{T}ZrP. Thus, the pH value has a slight influence on the adsorption capacity of ^{T}ZrP. The above results indicate that the existence of L-proline can assist in the adsorption of papain at a pH value lower than the p*I* of papain.

4. Conclusions

In summary, mesoporous zirconium organophosphonates with L-proline in the tunable mesopore were synthesized through the surfactant-assisted procedure. The organic solvents, THF, can effectively decrease the hydrolysis rate of the zirconium precursor to aid in the formation of mesoporosity of the resultant material. The pore size in the range of 4.8−16.3 nm can be easily controlled by adjusting the amounts of anionic surfactant (SDS) in the initial reactants. The most interesting is that a hierarchically mesoporous zirconium phosphate with a binary mesoporous structure can be obtained through calcination of mesoporous zirconium organophosphonate. The mesoporous zirconium organophosphonate with high surface area, large pore volume, and pore size exhibits high adsorption capacity and adsorption rate for the enzyme. The Lz adsorbed on the mesoporous zirconium organophosphonate has a structural conformation similar to that of its free state, suggesting that no denaturalization of Lz occurs during the adsorption process. Furthermore, no obvious leaching of Lz and papain from the mesoporous zirconium organophosphonate was observed. The mesoporous zirconium organophosphonates exhibit much higher adsorption amounts of papain at pH = 4.0 (pH < p*I* of papain) than at pH = 9.2 (pH > p*I* of papain) because of the existence of L-proline groups in the mesopores. The mesoporous zirconium phosphate (without the L-proline) has almost the same adsorption capacities at pH = 4.0 and 9.2.

Acknowledgment. Financial support of this work was provided by the National Natural Science Foundation of China (Grants 20503028, 20621063, and 20673113), Doctoral Research Foundation of Liaoning Province (Grant 20061055), and National Basic Research Program of China (Grants 2003CB615803 and 2005CB221407).

Supporting Information Available: SEM images. This material is available free of charge via the Internet at http://pubs.acs.org.

IC700892Z